

Trajectory Planning Technique Based on Curved-Layered and Parallel Contours for 6-DOF Deposition

Juan C. Guacheta-Alba , Sebastian Gonzalez , Mauricio Mauledoux , Oscar F. Aviles 
and Max Suell Dutra 

Abstract—The manufacture of solids using material deposition has boomed in recent years, and its use has grown steadily, generating challenges to improve printing. In addition, new mechanisms of six degrees of freedom have been designed focused on manufacturing parts, creating problems such as their trajectory planning. Therefore, this paper presents a new path-planning methodology based on the contour-parallel pattern and, through propagation techniques and geodesic flattening, transforms curved spaces into flat contours and vice versa. Furthermore, this methodology generates continuous trajectories for manufacturing parts for mechanisms of six degrees of freedom, focused on improving the surface quality and the quantity of deposited material, eliminating unwanted effects such as ladder and stringing, which usually occur in 3D printing.

Index Terms—Additive manufacturing, Curved-layered printing, Flattening, Trajectory planning.

I. INTRODUCTION

In additive manufacturing applications, a recently investigated topic is trajectory planning, which will describe the behavior of printing and the quality with which it will be developed. For this, several factors are considered, such as the surface finish, the density of the piece, the final mechanical properties that the printing part will present, and the type of curves that the extruder will describe [1], [2]. These trajectories have been obtained from two approaches: based on cartesian movements or parametric movements [3], [4].

The trajectories based on developed cartesian motions are the space-filling curves, as well as a variant of these which are the curves described in zigzag, in addition to the Hilbert curves, which belong to the group of continuous fractal curves. On the other hand, the trajectories based on parametric movements investigated have been the curves based on spirals, as well as the iso-contours or parallel contours which cover the area with geometries similar to the contours. This section presents a compilation of these techniques and some variants implemented [5]. The iso-contours or parallel contours are within trajectories based on parametric movements, which depend directly on the geometry to be filled [6]. For example, Fig. 1 shows the parallel contours of a square region, which

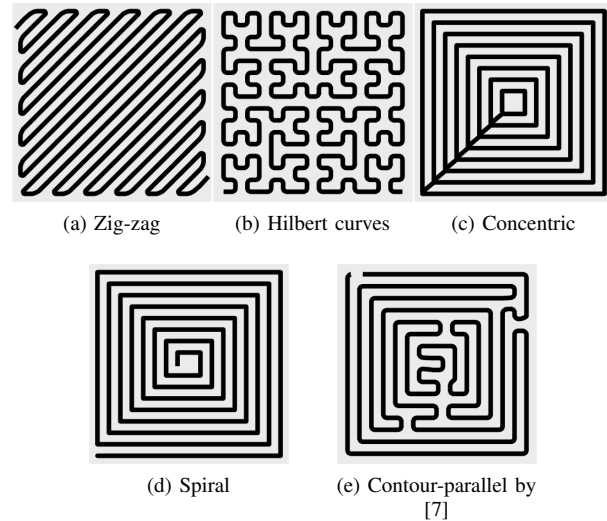


Fig. 1. Deposition patterns for additive manufacturing.

represent the same square geometry, but with a size reduction. Notably, these geometries are decreasing concerning the geometric center of the region to be analyzed [7].

Surface discretization allows expressing, using a set of points in space, a region of a continuous surface. This representation of surfaces is made employing the Voronoi diagram [8]. However, it is commonly done by polygonal meshing, where its following derivatives are used: rectangular meshing and triangular meshing [9]. Each of these presents different characteristics in its discrete approach. For example, the rectangular mesh can be constructed by projecting a mesh at its base. In addition, this meshing can generate a zigzag trajectory over the discretized points [10], [11].

On the other hand, other techniques are focused on flattening without fixed contour, possibly preserving the area and length of the meshing [12]. Some of them are the reverse forming of a step and the flattening based on angle, which can be seen in Fig. 2. These have higher computational costs in their development but manage to minimize the deformations of the process. These surface discretization techniques focus on material subtraction processes but apply to additive manufacturing [13], [14].

Finally, trajectorial planning has been extensively researched. However, its focus has been limited to layer-by-layer

Juan C. Guacheta-Alba and Max Suell Dutra are with Robotics Laboratory, Mechanical Engineering Department, Universidade Federal do Rio de Janeiro Brazil e-mail:email@mecanica.coppe.ufrj.br

Sebastian Gonzalez, Mauricio Mauledoux and Oscar F. Aviles are with Davinci Research Group, Mechatronics Engineering Department, Universidad Militar Nueva Granada Colombia e-mail:email@unimilitar.edu.co

Manuscript received March 03, 2023; revised March xx, 2023.

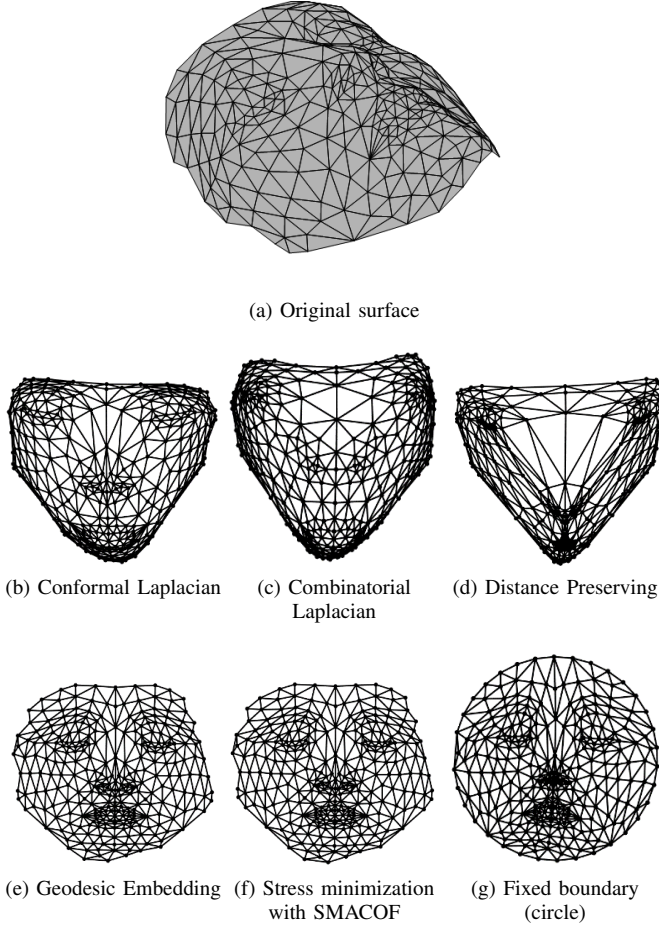


Fig. 2. Application of surface flattening techniques [15].

deposition processes in 3D printing systems with 3 degrees of freedom, restricting printing to cartesian movements. Although additive manufacturing systems with higher degrees of freedom have been investigated, they continue to use trajectory planning based on space-filling or zigzag movements. In addition, they have been shown to improve the surface quality of the manufactured part and reduce discarded support material and production time [16], [17]. Therefore, the proposed recent algorithms have been focused on 3D printing using a three-degree freedom machine, restricting the movements that can be developed with a six-degree freedom machine, including pitch, yaw, and roll, and depositing support material subsequently discarded in manufacturing [18].

This paper presents a new methodology for planning trajectories focused on additive manufacturing developed by mechanisms of six degrees of freedom with an input file of the piece in STL format, taking into account that it is the most used conventional format due to its ease of translation by 3D printers and its popularity. It is organized as follows: the method section defines the step by step of generating the trajectories, starting with the obtaining of curved layers, continuing with the process of flattening of layers, calculating of trajectory for each layer, and ending with its connection,

generating a continuous trajectory. Then, the case study section is presented, where five pieces are presented on which trajectories are calculated in the results and discussion section. Finally, these trajectories are discussed in this section, and it is finished with the conclusions section, where the advantages of the proposed new methodology are pointed out.

II. METHODS

A. Curved Layers Discretization

The objective is to implement a layer discretization system that considers each face's characteristics for each section or sub-volume of the piece. For this, as an initial step, it is sought to obtain the lower and upper curved layers for the pieces to be printed in order to use them to print the surface with the best surface finish, and in the same way, using them, make a propagation of its curvature and obtain the following layers that will form the piece to be printed, guaranteeing its equidistance and the correct filling of the solid.

When obtaining this surface, its main objective is its propagation respecting the equidistance between the previous and new surface, in addition to using the normal of each face to obtain the new surface [19]. The pseudoinverse matrix of the normal connected to each vertex is used, using Eq. (1). Due to the programming methodology, a new surface with propagation limitation is generated on the z-axis.

$$Propagation = \begin{cases} \begin{bmatrix} NormalVectors \\ 0 & 0 & -1 \end{bmatrix}^{-1} \cdot [1 \ 1 \ 0]^T & \text{if } Faces = 2 \\ [NormalVectors]^\dagger \cdot [1 \ 1 \ 1]^T & \text{if } Faces > 2 \end{cases} \quad (1)$$

Finally, a continuous propagation is carried out on the surface, as defined in Algorithm 1, in which a series of surfaces are obtained that fill the region to be printed. Fig. 3 shows the results of propagating the surface of a spherical hull. It is possible to visualize the equidistance between the generated layers. Because the direction of the faces has a counterclockwise sense due to the STL convention, the normal will always be directed towards the internal direction of the part, this principle being used in the direction of propagation of the curved layers [20].

Algorithm 1 Surface propagation

- 1: **Inputs:**
Vertices: Vertices of the piece
Faces: Faces of the piece
Tol: Area tolerance
 - 2: **Outputs:**
PropVertices: Propagated vertices
 - 3: *ReducedFaces* \leftarrow Reduce *Faces* with area less than *Tol*
 - 4: *Normal* \leftarrow Calculate normal of *ReducedFaces*
 - 5: *#Vertices* \leftarrow Number of *Vertices* of the piece
 - 6: **for** $i \leftarrow 1$ to *#Vertices* **do**
 - 7: *VerticesDirection* \leftarrow Inverse of the normal of *Faces* connected to *Vertices*, using Eq. (1)
 - 8: *VerticesDistance* \leftarrow *VerticesDirection* \div length of *VerticesDirection* $\cdot 0.4mm$
 - 9: *PropVertices* \leftarrow *VerticesDistance* + *Vertices*
 - 10: **end for**
-

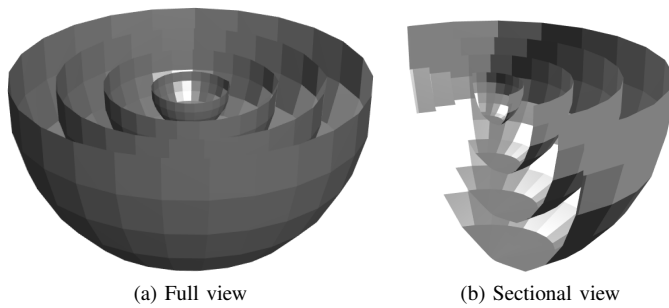


Fig. 3. Lower surface propagation for spherical model.

B. Flattening

An approximation that has been made previously is the transformation of flat layers. Still, with angles of rotation that respect the orientation of the geometry being novel in the printing process, it is desired to expand the printing process taking into account thoroughly the surface finish of the piece [21].

1) *Direct Flattening*: Several flattening techniques have been investigated. They seek to minimize a cost function that penalizes area distortion, changes in geodesic distance, or, more commonly, a combination of different distortion measures [22]. The round contour face model is an example to compare the yields of conventional methods. The Gaussian curvature is high in the nose, mouth, and eyes parts of the original model. Therefore, it is easier to unfold them with distortion [23]. The model flattening result is performed for the following proposed methods: circular boundary conformal flattening, free-limit conforming flattening, the spectral flattening method, and the iso map flattening method are shown in Fig. 2 [24]. In order to compare the six flattening techniques mentioned, the perimeter ratio of the original model and the flattened model is defined, which is defined in Eq. (2).

$$DeformationMetric = \sum_{n=1}^{Faces} \left| 1 - \frac{Perimeter_{FlattenedFace}^n}{Perimeter_{OriginalFace}^n} \right| \quad (2)$$

As can be seen in Table I, the stress minimization flattening technique is the one that performs best on the mean square error metric calculated for each of the triangles of the mesh, followed by the geodesic transformation, which is in the same range of results as the first, the latter being the one used in the flattening of surfaces. These results are presented in Table I, which corroborates the low deformation of perimeters using geodesic flattening techniques and stress minimization.

Geodesic flattening is a technique of converting a smooth surface into a flat surface based on calculating the shortest path in each triangular mesh and then performing the iterative computation of a global geodesic [25]. On this geodesic, which is expressed in a matrix of distances, the eigenvalues and eigenvectors are calculated that allow the transformation of the vertices of the surface. This flattening is premised in that it ensures that each segment found on each of the surface faces now becomes almost straight instead of curved nature [26], [27]. Algorithm 2 is based on the codes and functions

Algorithm 2 Geodesic flattening

```

1: Inputs:
   Vertices: Vertices of the surface
   Faces: Faces of the surface
2: Outputs:
   FlatVertices: Flattened vertices of the surface
3: #Vertices ← Number of Vertices of the surface
4: D ← zeros 2D array of size #Vertices
5: for i ← 1 to #Vertices do
6:   D(i) ← perform fast-moving mesh with Vertices, Faces
   and i
7: end for
8: D ← (D + D') ÷ 2
9: J ← identitymatrix − onematrix ÷ #Vertices
10: S ← vector of eigenvalues of W
11: U ← matrix of eigenvalues of W, where W * U = U * S
12: U ← sort U by eigenvalues descending
13: T ← square root of two first eigenvalues
14: FlatVertices ← U' * T

```

TABLE I

DEFORMATION EVALUATION FOR FLATTENING METHODS.

Method	Deformation metric [mm]
Conformal Laplacian	185.7682
Combinatorial Laplacian	220.5868
Distance Preserving	284.1212
Geodesic Embedding (Isomap)	30.6648
Stress minimization with SMACOF	28.8433
Fixed boundary (circle)	81.7807

programmed by [15], who provides a complete MATLAB® toolbox for flattening mesh surfaces.

2) *Inverse Flattening*: In this section, the calculation of a printing path on the curved surface will be carried out using the flattening techniques mentioned in the previous section and the programming of an inverse function to the flattening process. As a primary objective, the use of flattening of the meshed surface is sought, and find the trajectory that the filling would make on it. For this, Eq. (3) is defined, where two director vectors are used for each face, both the flattened, with subscript A, and the original, with subscript B. This equation transforms the trajectory within the flattened triangle and performs a rotation to obtain this trajectory on the original surface.

$$T_{R_B} = V \vec{d}_B \cdot V \vec{d}_A^{-1} \cdot T_{R_A} \quad (3)$$

Finally, with the contour calculation on the flattened mesh, a test path vector is obtained for the contour obtained to calculate connections between them. Calculating the trajectories to fill the piece on these contours is facilitated. For this, the respective connections of the parallel contours for the already flattened surface is carried out, as well as the smoothing process to improve the printing process of the part and the operation of the machine. The complete methodology of inverse flattening is expressed in Algorithm 3.

C. Closed Path in Layer

Based on the parallel contours, and taking into account the problem that they are not continuous trajectories that they generate, two methodologies of connection between these

Algorithm 3 Inverse flattening on 2D surfaces

```

1: Inputs:
   OVertices: Vertices of the original surface
   FVertices: Vertices of the flattened surface
   Faces: Faces of the surface
   FTray: Trajectory obtained on the flattened
   surface
2: Outputs:
   OTray: Trajectory obtained on the original surface
3: #Faces  $\leftarrow$  Number of Faces of the surface
4: for i  $\leftarrow$  1 to #Faces do
5:   ActualTrajectory  $\leftarrow$  select the trajectory section within
   triangle i
6:   if ActualTrajectory is not empty then
7:     CenteredTrajectory  $\leftarrow$  ActualTrajectory -
     ThirdOriginalVertex
8:     OriginalDirections  $\leftarrow$  FirstOriginalVertex
     - ThirdOriginalVertex and SecondOriginalVertex -
     ThirdOriginalVertex
9:     FlatDirections  $\leftarrow$  FirstFlatVertex
     - ThirdFlatVertex and SecondFlatVertex -
     ThirdFlatVertex
10:    RotatedTrajectory  $\leftarrow$  OriginalDirections  $\cdot$ 
    FlatDirections-1  $\cdot$  CenteredTrajectory +
    ThirdOriginalVertex, using Eq. (3)
11:    FinalTrajectory  $\leftarrow$  locate ActualTrajectory on
    FinalTrajectory
12:  end if
13: end for
    
```

closed curves are proposed, based mainly on the cut of each contour, its contiguous contour, and its union using lines. For these methodologies, the connection is made from the internal contour and continues towards the external. As a first option, the following steps in the generation are proposed: initially, the internal contour is selected, a random cut is made with a distance corresponding to the thickness of the nozzle, and after this, the tangent line to the contour is calculated at the selected points; With these lines, the cuts of these are sought in the contiguous contour, and a line makes their connection. Once this process has been carried out in the first contour, these steps are carried out cyclically in all the contours. A visualization of the developed process, using the techniques of direct and reverse flattening for a spherical cap is presented in Fig. 4, for more information on the trajectory generation, it is recommended to consult reference [7].

D. Connecting Layers

Based on the previous method, and considering that they have closed trajectories in each layer, a methodology of connection between these curves is proposed based mainly on the cut of each trajectory per layer, its contiguous layer, and its union employing lines. For this methodology, the connection is made from the lower contour and continues toward the upper one, and a representation of connection between two layers for a cap is presented in Fig. 5.

E. Path Planning

The following steps are proposed in the generation: initially, the internal contour is selected, and a random cut is made with a distance corresponding to the thickness of the nozzle.

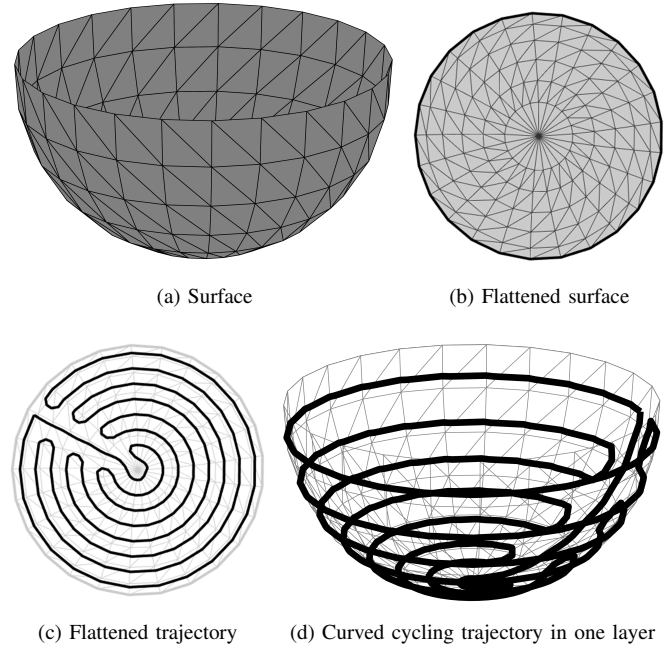


Fig. 4. Trajectory planning methodology for spherical surface.

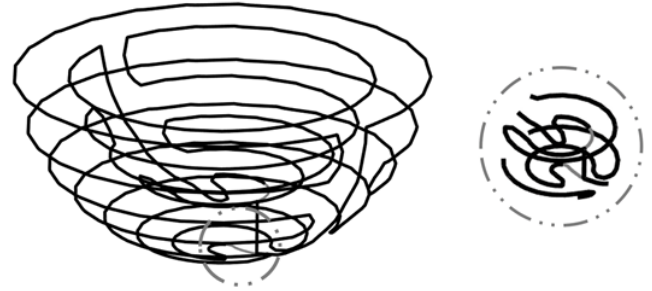


Fig. 5. Visualization of connection of trajectories between curved layers.

After this, the tangent line to the contour is calculated at the selected points; With these lines, the cuts of these are sought in the contiguous contour, and a line makes their connection. Once this process has been carried out in the first contour, these steps are carried out cyclically in all the contours [28], [29]. This process is detailed in Algorithm 4, which expresses the cyclical process of each method and algorithm developed previously to find the final complete continuous trajectory.

Thus, summarizing, this section has presented the methodology used to generate trajectories for mechanisms with six degrees of freedom, starting with a process of curved discretization based on geometry, then a flattening process based on geodesic flattening, and a calculation of trajectory per layer based on parallel contours, as shown in Fig. 4. Finally, an inverse flattening process is performed, and each curved path per layer is connected to generate a single continuous fill print path.

Algorithm 4 Trajectory planning routine

```

1: Inputs:
   Piece: 3D model
   Tol: Area tolerance
2: Outputs:
   PTray: Printable path for 3D model
3: Vertices; Faces  $\leftarrow$  read Piece in format STL
4: while Piece is not fill by surfaces do
5:   PropagatedVertices  $\leftarrow$  SurfacePropagation(Vertices, Faces, Tolerance)
6:   #Layers ++
7: end while
8: for i  $\leftarrow$  1 to #Layers do
9:   FlatLayer  $\leftarrow$  Geodesic flattening for i-th layer
10:  FlatTrajectory  $\leftarrow$  creation of close path in FlatLayer
11:  TrajectoryInLayer  $\leftarrow$  Inverse flattening on 2D surfaces
    of FlatTrajectory
12: end for
13: PTray  $\leftarrow$  connect TrajectoryInLayer

```

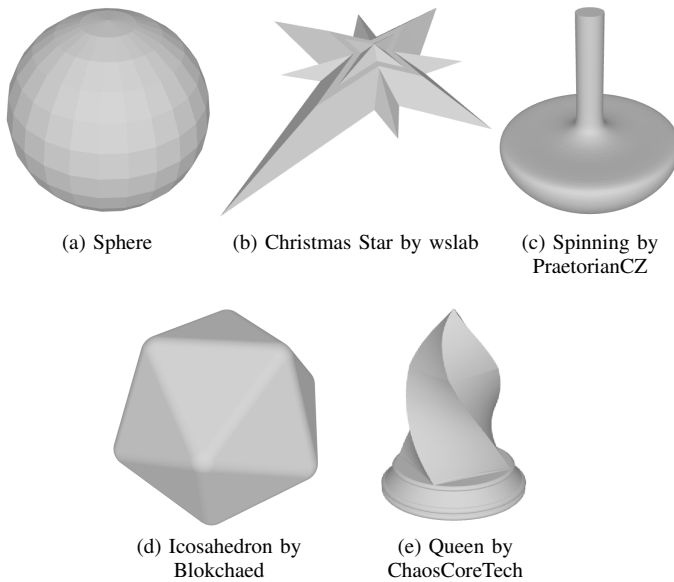


Fig. 6. Selected part models.

III. CASE STUDY

A gallery of 5 pieces is selected, which will generate challenges and evaluate the correct functioning of the trajectory generation algorithm. The pieces, presented in Fig. 6, are taken from web repositories with a Creative Commons CC license. The diversity of geometries in the selected parts allows to observe and analyze different characteristics in the generation of trajectories, using processes of the plane and curved discretization, both separately and in combination. Another essential aspect to mention about the selected pieces is the number of faces and vertices that compose them since this may facilitate or complicate the generation and evaluation of trajectories. For this study, a filling percentage of 100% is proposed. However, it is mentioned that, as presented in [7], this technique can vary the distance of the contours to modify the filling percentage.

IV. RESULTS AND DISCUSSION

The trajectory generation methodology presented in the method section is applied to various geometries that allow evaluating their potential in the face of challenges such as concave and convex surfaces and models with a high number of faces, as well as miniature models that need high precision. Table II compiles the volume and dimensions information of each model used and the amount of material calculated for each model. It is mentioned that, for the calculated trajectories, a nozzle diameter for the printing of 0.4 mm is considered, being a commercial dimension. Therefore, various dimensions can be observed, from models with a height of 1.97 mm to heights of 4 mm and models with a volume to cover small, which will require high precision and which, with conventional printing in 3D printing, they will present a high presence of staggered layers.

Fig. 7 shows the trajectories obtained for the five pieces selected in the case study. The scales selected for the pieces are low to present a correct visualization of the trajectories and greater complexity due to the precision needed. However, this procedure can be scalable to models of parts with larger dimensions, with similar results. On average, seven layers were used for the models to fill each model. For some models, mixed layer creation processes were used in sections with no curvature, and flat layers are required, as in the base of the model Queen by ChaosCoreTech and in the upper section of the model Spinning by PraetorianCZ. The trajectories gener-

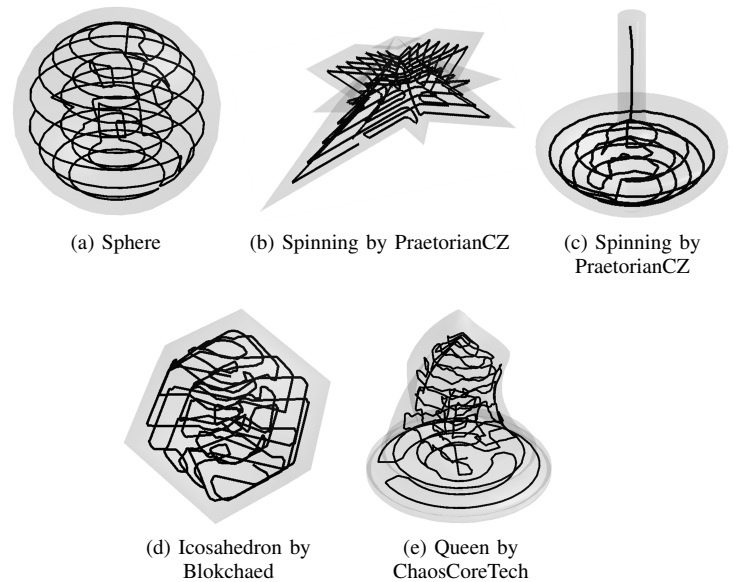


Fig. 7. Trajectories obtained in selected part models.

ated are continuous, without pauses in the material deposition. Therefore, at the time of printing generates the phenomenon of stringing, which consists of deformed material affecting print quality. In addition, since it is a continuous trajectory, the printing time is minimized compared to conventional trajectory generation techniques, which can be observed in the video here for better visualization. This proposed new method was based on generating trajectories for a parallel kinematics

TABLE II
INFORMATION REGARDING PRINTING PARTS.

Parts	Volume [mm^3]	Deposited material [mm]	Size [mm]
Sphere	16.809	141.43	[3.20 – 3.20 – 3.20]
Christmas Star by wslab	21.816	182.02	[10.03 – 12.85 – 1.97]
Spinning by PraetorianCZ	8.176	62.03	[3.31 – 3.31 – 3.83]
Icosahedron by Blokchaed	11.459	91.38	[3.16 – 2.80 – 2.64]
Queen by ChaosCoreTech	11.230	89.76	[3.32 – 3.32 – 3.94]

mechanism of six degrees of freedom. However, its results can be implemented on six serial degrees of freedom systems. Furthermore, in some situations where the inclination of the layers is not high, as in the Star by Arty model, these paths can be implemented in conventional three-degree-of-freedom printers.

V. CONCLUSIONS

The realization of an algorithm for planning the trajectories of the machine is proposed. Similar to the 3D printing process, this project receives any object in STL format to be processed by the system and exports the coordinates of the print path. Their approach is based on sending data to a 6DOF robot with a MATLAB connection, but it can be exported to G-CODE format used by commercial software. Then, the geometric analysis of the pieces is carried out by detecting the lower and upper surfaces, exposed in method section, together with their cyclic propagation that fills the solid to be built. The technique of geodesic flattening is applied to make the transition of surfaces in a curved space to a flat one, which presents the least deformations of the space, being a fundamental criterion for the transformation of trajectories. The complete discretization system is structured in Algorithm 1, where the resources of plane discretization, curve propagation, and direct and inverse flattening are exploited. As a result, these trajectories, when filling layer by layer, are entirely connected, generating a single filling path for a specific part, eliminating travel displacements, achieving a deposition of material continuously and without interruptions, and improving the quality of the surface finish. These trajectories obtained, in turn, reduce the printing time of the pieces. Also, due to the deposition of material with six degrees of freedom, problems such as the staircase effect and z-wobble that are easily presented in 3D printing are eliminated, directly affecting the surface quality of the piece. Likewise, another advantage of the designed trajectories is that, given their continuity and that no braking will be carried out in the deposition of material, effects such as stringing, which occurs when in the same layer there are sections with unwanted material since a travel movement is made there, are eliminated, improving the quality of the piece obtained. Given that there are selected process parameters, such as filling, printing speed, and pattern type, which affect the quality of the part and its structural behavior, in future work, it is proposed to optimize the trajectory planning methodology by defining decision strategies and KPIs [30]. In turn, the STL format has been used to read objects, given its constant use in printing.

However, it is proposed to extend the methodology to new formats such as STEP, 3MF, and OBJ, improving the accuracy of calculating trajectories.

ACKNOWLEDGEMENTS

This paper is a research product from the IMP-ING-3122 high-impact project funded by the Research Vice-Chancellor of Universidad Militar Nueva Granada–2022. Producto derivado del Proyecto IMP-ING-3122 financiado por la Vicerrectoría de Investigaciones de la Universidad Militar Nueva Granada–Vigencia 2022.

REFERENCES

- [1] T. Vaneker, A. Bernard, G. Moroni, I. Gibson, and Y. Zhang, “Design for additive manufacturing: Framework and methodology,” *CIRP Annals*, vol. 69, no. 2, pp. 578–599, 2020.
- [2] A. Mostafaei, A. M. Elliott, J. E. Barnes, F. Li, W. Tan, C. L. Cramer, P. Nandwana, and M. Chmielus, “Binder jet 3d printing—process parameters, materials, properties, modeling, and challenges,” *Progress in Materials Science*, vol. 119, p. 100707, jun 2021.
- [3] A. Nazir, K. M. Abate, A. Kumar, and J.-Y. Jeng, “A state-of-the-art review on types, design, optimization, and additive manufacturing of cellular structures,” *The International Journal of Advanced Manufacturing Technology*, vol. 104, pp. 3489–3510, jul 2019.
- [4] A. Gubankov and I. Gornostaev, “Comparison study of different types of setting reference movements for mechatronic objects by parametric splines,” in *2022 International Conference on Ocean Studies (ICOS)*, IEEE, oct 2022.
- [5] K. L. Ameta, V. S. Solanki, V. Singh, A. P. Devi, R. Chundawat, and S. Haque, “Critical appraisal and systematic review of 3d and 4d printing in sustainable and environment-friendly smart manufacturing technologies,” *Sustainable Materials and Technologies*, vol. 34, p. e00481, dec 2022.
- [6] D. Zhao and W. Guo, “Shape and performance controlled advanced design for additive manufacturing: A review of slicing and path planning,” *Journal of Manufacturing Science and Engineering*, vol. 142, nov 2019.
- [7] J. C. Guacheta-Alba, D. A. Nunez, M. Mauledoux, and O. F. Aviles, “Deposition toolpath pattern comparison: Contour-parallel and hilbert curve application,” *International Journal of Mechanical Engineering and Robotics Research*, pp. 542–548, 2022.
- [8] B. Zhou, T. Tian, J. Zhao, and D. Liu, “Tool-path continuity determination based on machine learning method,” *The International Journal of Advanced Manufacturing Technology*, vol. 119, pp. 403–420, nov 2021.
- [9] W. Xu, H. Xu, Q. Li, P. Zhang, L. Yang, and W. Wang, “Stress-based path planning on quad mesh for additive manufacturing,” *SSRN Electronic Journal*, 2022.
- [10] J. Xu, Y. Sun, and L. Zhang, “A mapping-based approach to eliminating self-intersection of offset paths on mesh surfaces for CNC machining,” *Computer-Aided Design*, vol. 62, pp. 131–142, may 2015.
- [11] H. Zhang, Y. Yao, Y. Ma, M. Lackner, and Y. Jiang, “A 3d printing tool-path generation strategy based on the partition of principal stress field for fused filament fabrication,” *The International Journal of Advanced Manufacturing Technology*, vol. 122, pp. 1719–1735, aug 2022.
- [12] F. Liang, C. Kang, Z. Lu, and F. Fang, “Iso-scallop tool path planning for triangular mesh surfaces in multi-axis machining,” *Robotics and Computer-Integrated Manufacturing*, vol. 72, p. 102206, dec 2021.

- [13] A. Bacciaglia, A. Ceruti, and A. Liverani, "A systematic review of voxelization method in additive manufacturing," *Mechanics and Industry*, vol. 20, no. 6, p. 630, 2019.
- [14] C. Tomassoni, O. A. Peverini, G. Venanzoni, G. Addamo, F. Paonessa, and G. Virone, "3d printing of microwave and millimeter-wave filters: Additive manufacturing technologies applied in the development of high-performance filters with novel topologies," *IEEE Microwave Magazine*, vol. 21, pp. 24–45, jun 2020.
- [15] G. Peyré, "The numerical tours of signal processing," *Computing in Science and Engineering*, vol. 13, pp. 94–97, jul 2011.
- [16] M. Mehrpouya, A. Dehghanghadikolaei, B. Fotovvati, A. Vosooghnia, S. S. Emamian, and A. Gisario, "The potential of additive manufacturing in the smart factory industrial 4.0: A review," *Applied Sciences*, vol. 9, p. 3865, sep 2019.
- [17] J. Jiang, X. Xu, and J. Stringer, "Optimization of process planning for reducing material waste in extrusion based additive manufacturing," *Robotics and Computer-Integrated Manufacturing*, vol. 59, pp. 317–325, oct 2019.
- [18] H. Zeng, M. Feng, J. Zhuang, R. Cai, Y. Xie, and J. Li, "3d printing and free-form surface coating based on 6-DOF robot," in *2019 IEEE International Conference on Robotics and Biomimetics (ROBIO)*, IEEE, dec 2019.
- [19] D. Kraljić and R. Kamnik, "Trajectory planning for additive manufacturing with a 6-DOF industrial robot," in *Advances in Service and Industrial Robotics*, pp. 456–465, Springer International Publishing, sep 2018.
- [20] Y. Weng, N. A. N. Mohamed, B. J. S. Lee, N. J. H. Gan, M. Li, M. J. Tan, H. Li, and S. Qian, "Extracting BIM information for lattice toolpath planning in digital concrete printing with developed dynamo script: A case study," *Journal of Computing in Civil Engineering*, vol. 35, may 2021.
- [21] Y.-L. Cheng, C.-H. Chang, and C. Kuo, "Experimental study on leveling mechanism for material-jetting-type color 3d printing," *Rapid Prototyping Journal*, vol. 26, pp. 11–20, jan 2020.
- [22] S. M. Abulnaga, E. A. Turk, M. Bessmeltsev, P. E. Grant, J. Solomon, and P. Golland, "Placental flattening via volumetric parameterization," in *Lecture Notes in Computer Science*, pp. 39–47, Springer International Publishing, 2019.
- [23] Y. Kita and N. Kita, "Virtual flattening of a clothing surface by integrating geodesic distances from different three-dimensional views," in *Proceedings of the 14th International Joint Conference on Computer Vision, Imaging and Computer Graphics Theory and Applications, SCITEPRESS - Science and Technology Publications*, 2019.
- [24] M. Budninskiy, G. Yin, L. Feng, Y. Tong, and M. Desbrun, "Parallel transport unfolding: A connection-based manifold learning approach," *SIAM Journal on Applied Algebra and Geometry*, vol. 3, pp. 266–291, jan 2019.
- [25] P.-F. Zheng, Q. Liu, J.-D. Zhao, D.-J. Lin, and Q. An, "An algorithm for computing geodesic curve based on digital experiment of point clouds," in *Advances in Intelligent Systems and Computing*, pp. 2282–2294, Springer International Publishing, jul 2018.
- [26] D. Sarkar and K. Deyasi, "Computing the geodesic distance between two points in a polyhedral solid," *International Journal of Advanced Science and Engineering*, vol. 6, pp. 21–24, jul 2019.
- [27] K. Crane, M. Livesu, E. Puppo, and Y. Qin, "A survey of algorithms for geodesic paths and distances," 2020.
- [28] K. Huang, H. Gong, and X. Chen, "Study of ultra-precision turning path calculation of freeform surface with free contours," *The International Journal of Advanced Manufacturing Technology*, vol. 121, pp. 5451–5462, jul 2022.
- [29] H.-Y. Ma, C.-M. Yuan, and L.-Y. Shen, "Tool path planning with confined scallop height error using optimal connected fermat spirals," *Communications in Mathematics and Statistics*, nov 2022.
- [30] P. Stavropoulos, K. Tzimanis, T. Souflas, and H. Bikas, "Knowledge-based manufacturability assessment for optimization of additive manufacturing processes based on automated feature recognition from cad models," *The International Journal of Advanced Manufacturing Technology*, vol. 122, pp. 993–1007, Sep 2022.



Juan C. Guacheta-Alba received his B.S. in mechatronics engineering from Universidad Militar Nueva Granada in 2020 and his M.Sc. in mechatronics engineering from Universidad Militar Nueva Granada in 2022. Currently, he is working toward the Ph.D. in mechanical engineering at Universidade Federal do Rio de Janeiro. His research interests include robotics, multi-agent systems and optimization. He can be contacted at email: est.juan.guacheta@unimilitar.edu.co.



Sebastian Gonzalez received his B.S. in mechatronics engineering from Universidad Militar Nueva Granada in 2020. Currently, he is working toward the M.Sc. degree in Mechatronics Engineering at Universidad Militar Nueva Granada. His research interests include optimization and robotics. He can be contacted at email: est.sebastian.gonzal@unimilitar.edu.co.



Mauricio Mauledux received his B.S. in mechatronics engineering from Universidad Militar Nueva Granada, in 2005. In 2011, he received his PhD degree in Mathematical models, numerical methods, and software systems (Red Diploma) from St. Petersburg State Polytechnic University, Russia. In 2012, he joined the Department of Mechatronic Engineering, at Universidad Militar Nueva Granada, in Colombia as Assistant Professor. His current research interests include robotics, automatic control, multi-agent systems, smart grids, and optimization.

He can be contacted at email: mauricio.mauledux@unimilitar.edu.co.



Oscar F. Aviles received his B.S. in electronics engineering from Universidad Antonio Nariño, in 1995. He received his PhD degree in Mechanical Engineering (Robotics Devices) in 2008 from Universidade Estadual de Campinas, Brazil. In 1998, he joined the Department of Mechatronics Engineering at Universidad Militar Nueva Granada, Colombia. His current research interests include robotics and biomechanics. He can be contacted at email: oscar.aviles@unimilitar.edu.co.



Max Suell Dutra received the B.S. degree in Mechanical Engineering from Federal University Fluminense, Rio de Janeiro, Brazil in 1987, M.Sc. degree in Mechanical Engineering from Federal University of Rio de Janeiro, Rio de Janeiro, Brazil in 1990, and Dr.-Ing. Degree from Gerhard Mercator Universität, Duisburg, Germany, 1995. Since 1999, he has been an Assistant Professor with the Mechanical Engineering Department, Federal University of Rio de Janeiro. He is the author of one book, more than 200 articles. His research interests include

mechatronic systems design, analysis of engineering disasters, robotics, instrumentation, industrial automation, biomechanics, nonlinear dynamics and multi-body systems. He can be contacted at email: max@mecanica.coppe.ufrj.br